

Finding and Editing Multi-Modal Neurons in Pre-Trained Transformer

Haowen Pan¹, Yixin Cao², Xiaozhi Wang³, Xun Yang^{1*}

¹University of Science and Technology of China

²Singapore Management University

³Tsinghua University

phw1129@mail.ustc.edu.cn, caoyixin2011@gmail.com

wangxz20@mails.tsinghua.edu.cn, xyang21@ustc.edu.cn

Abstract

Multi-modal large language models (LLM) have achieved powerful capabilities for visual semantic understanding in recent years. However, little is known about how LLMs comprehend visual information and interpret different modalities of features. In this paper, we propose a new method for identifying *multi-modal neurons* in transformer-based multi-modal LLMs. Through a series of experiments, We highlight three critical properties of multi-modal neurons by four well-designed quantitative evaluation metrics. Furthermore, we introduce a knowledge editing method based on the identified multi-modal neurons, for modifying a specific token to another designative token. We hope our findings can inspire further explanatory researches on understanding mechanisms of multi-modal LLMs.

1 Introduction

Recently, large language models (LLMs) have received much attention and become a foundation model in many natural language processing applications (Du et al., 2022; Touvron et al., 2023a; Chiang et al., 2023; Geng et al., 2023). Following the success, researchers in the area of computer vision have extended the input modality to both text and image, namely multi-modal LLMs, showing remarkable performance in various visual understanding tasks, such as MiniGPT-4 (Zhu et al., 2023), LLaVA (Liu et al., 2023), InstructBLIP (Dai et al., 2023) and mPLUG-Owl (Ye et al., 2023). Nevertheless, the underlying mechanism of how multi-modal LLMs abstract and interpret different modalities of features beyond these tasks remains unclear. This not only hinders in-depth investigation, but also poses risks in multi-modal LLMs applications, such as producing misleading outputs without insight into decisions, propagating biases through automatic captions, and reducing oversight for harmful outputs.

Many existing works align the internal states of LLMs with natural language for interpretability, e.g., by finding the processes of how facts are stored and accessed in a way that allows for changes and corrections (Meng et al., 2022, 2023), quantifying the uncertainty, misinformation and hallucination of LLM predictions (Huang et al., 2023; Duan et al., 2023), or discussing the influence of in-context learning on model behavior (Olsson et al., 2022; Merullo et al., 2023), while only a few focus on multi-modal LLMs. As some works (Meng et al., 2022, 2023; Dai et al., 2022; Merullo et al., 2023) reveal that LLMs’ ability to understand textual information mainly comes from feed-forward networks (FFN), Schwettmann et al. (2023) identifies specific FFN neurons based on gradients, where these neurons play an important role in understanding images and generating textual description. They are named multi-modal neurons. Clearly, multi-modal neurons elucidate multi-modal LLMs’ ability to bridge visual and textual representations, being the key for interpretability.

In this paper, we propose a new method to identify multi-modal neurons in multi-modal LLMs and design metrics for quantitative analysis, including semantic sensitivity, position invariance, cross-images invariance and specificity. Based on extensive experiments, we have verified three critical properties: (1) **Sensitivity**. Multi-modal neurons are sensitive to particular concepts. Once they are activated by some regions of the input image, they are responsible for generating corresponding textual concepts. More importantly, these neurons are invariant in visual translation and to different inputs. (2) **Specificity**. Although different multi-modal neurons can be activated by the same concept, they are selectively active for these concepts and hardly respond to others. (3) **Causal-effect**. Multi-modal neurons and the associated concepts have causal-effect and are stable to perturbation. We carefully perturb and modify the identified

*Corresponding author.

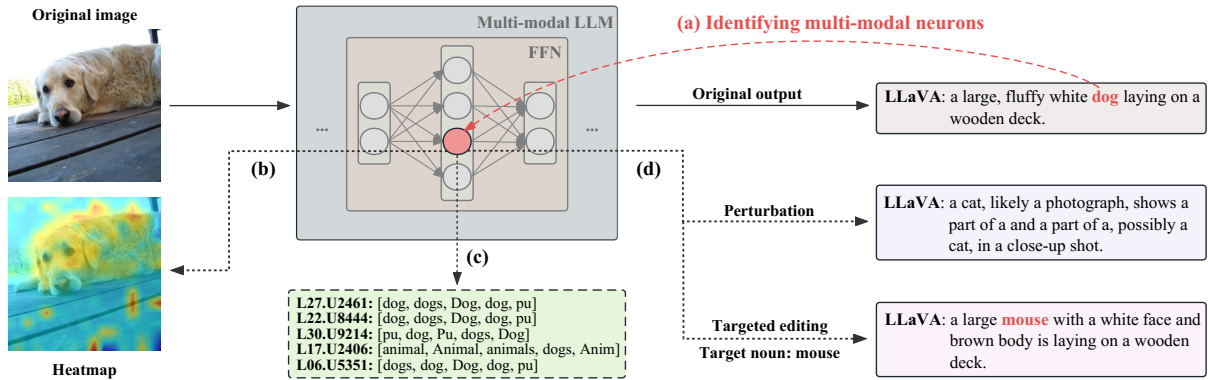


Figure 1: Multi-modal neurons in FFN within multi-modal LLM. We develop a method to (a) identify multi-modal neurons and confirm that they can encode specific concepts from (b) images to (c) texts and (d) causally affect model output.

multi-modal neurons, which leads to significant changes in the outputs, even gibberish. That is, a simple attack on several neurons may greatly break the ability of multi-modal LLMs to understand and interpret images.

Furthermore, we introduce a knowledge editing method based on the identified multi-modal neurons. We achieve the goal of modifying a specific token to another designative token, which is hoped to inspire future research such as automatically detecting and replacing sensitive information or identifiers in images, avoiding prohibited terms or phrases for legal and regulatory requirements.

Our contributions can be summarized as follows:

- We propose a new method for identifying multi-modal neurons in transformer-based multi-modal LLMs.
- We highlight three critical properties of multi-modal neurons by designing four quantitative evaluation metrics and extensive experiments.
- We propose a knowledge editing method based on the identified multi-modal neurons.

2 Method

We first introduce the architecture of multimodal large language models (§2.1) and neurons in Transformer (§2.2), and then expound how to identify multi-modal neurons in Transformer-based multi-modal large language models (§2.3) and trace the focus of neurons in images (§2.4). We also propose an efficient algorithm to transform a source token to another token when generating captions (§2.5). Furthermore, we measure a number of quantitative indicators to evaluate our selected neurons (§2.6).

2.1 Multimodal Large Language Models

Based on Transformer architecture, multimodal large language models have achieved powerful capabilities for visual semantic understanding (Li et al., 2023; Zhu et al., 2023; Liu et al., 2023; Ye et al., 2023). They generally consist of a visual encoder, a projection layer and a large language model (LLM). The visual encoder receives images and divides them into several small image patches, and then extracts image features as outputs. We denote the visual encoder outputs as $\mathcal{F} \in \mathbb{R}^{k \times d_h}$, where k is the number of image patches and d_h is the hidden size of the visual encoder. Through the projection layer, the image features \mathcal{F} are aligned into the textual prompt embeddings, which we denoted as $\mathcal{F}' \in \mathbb{R}^{k \times h}$, where h is the hidden size of the LLM. Ultimately, the aligned image features, concatenated with textual prompt embeddings, will be fed into the LLM, and the LLM will automatically decode the image features and provide a corresponding response.

2.2 Neurons in Transformer

A decoder-only Transformer (Vaswani et al., 2017) typically consists of stacked self-attention and feed-forward layers. Each layer first performs multi-head self-attention and then applies a position-wise feed-forward network (FFN). Residual connections and layer normalization are employed around each sub-layer. Following previous works (Dai et al., 2022; Wang et al., 2022; Schwettmann et al., 2023), we research the neurons within FFN, as the FFN carries two-thirds of the parameters and contains abundant information and knowledge. We denote the hidden states at layer l as \mathbf{h}^l , FFN output as \mathbf{m}^l and self-attention output \mathbf{a}^l , respectively. \mathbf{m}^l can

be calculate by:

$$\mathbf{m}^l = \mathbf{W}_{\text{out}}^l \sigma \left(\mathbf{W}_{\text{in}}^l \left(\mathbf{a}^l + \mathbf{h}^{l-1} \right) \right), \quad (1)$$

where \mathbf{h}_t^0 is the embedding vector of input, σ is the activation function, \mathbf{W}_{in}^l is the first linear layer and $\mathbf{W}_{\text{out}}^l$ is the second linear layer in FFN.

For simplicity, let $\mathbf{O}^l = \sigma \left(\mathbf{W}_{\text{in}}^l \left(\mathbf{a}^l + \mathbf{h}^{l-1} \right) \right)$, where the i -th element is regard as activation output of the i -th neuron. We denote each neuron in the LLM as $(Ll.Ui)$ in subsequent experiments.

2.3 Identifying Multi-Modal Neurons

We now introduce a contribution score that indicates a neuron’s contribution to a single token. By ranking the contribution scores, we can identify neurons within the model that are more contributive to specific tokens. Let \mathcal{M} be the LLM, \mathbf{x} be the sequence of input tokens and \mathbf{y} be the output sequence. The function of LLM can be written as:

$$\mathbf{y} = \mathcal{M}(\mathbf{x}). \quad (2)$$

Based on Eq. 1, we denote $\mathbf{Q}^l = \mathbf{W}_u \mathbf{W}_{\text{out}}^l \cdot \mathcal{T}(\mathbf{O}_{-1}^l) \in \mathbb{R}^{d_m \times v}$, where \mathbf{W}_u is the unembedding matrix to decode last hidden states, $\mathcal{T}(\cdot)$ is the transpose of the input matrix, \mathbf{O}_{-1}^l is the activation output at the last token, d_m is the intermediate size and v is the vocab size. We assume the model absorbs in the aligned image feature \mathcal{F}' and now is about to output token $t \in \mathbf{y}$, whose probability is maximum among the token vocabulary. Then we define the contribution score as below:

$$s_{i,t}^l = \mathbf{Q}^l(i, t), \quad (3)$$

which means when the model is predicting token t as its output, the contribution score of neuron u_i at layer l is $s_{i,t}^l$.

To prove rationality and effectiveness of our proposed method, we try to disassemble and deduce the generation procedure of the LLM. When a L layer Transformer-based LLM is generating a new token $t \in \mathbf{y}$, the probability distribution of output can be denoted as follows:

$$t = \operatorname{argmax} \left(\mathbf{W}_u \mathbf{h}_{-1}^L \right), \quad (4)$$

where \mathbf{W}_u is the unembedding matrix and \mathbf{h}_{-1}^L is the output of the last token at last layer L .

At layer l , we can decompose the hidden state \mathbf{h}_{-1}^l into three parts:

$$\mathbf{h}_{-1}^l = \mathbf{a}_{-1}^l + \mathbf{m}_{-1}^l + \mathbf{h}_{-1}^{l-1}, \quad (5)$$

where \mathbf{a}_{-1}^l and \mathbf{m}_{-1}^l is the self-attention and FFN output of the last token at layer l , respectively, \mathbf{h}_t^0 is the embedding vector of the input token $x_t \in \mathbf{x}$, and σ is the activation function.

Now Eq. 4 can be rewritten as below:

$$\begin{aligned} t &= \operatorname{argmax} \left(\mathbf{W}_u \left(\mathbf{a}_{-1}^L + \mathbf{m}_{-1}^L + \mathbf{h}_{-1}^{L-1} \right) \right) \\ &= \operatorname{argmax} \left(\sum_{l=1}^L \left(\mathbf{W}_u \mathbf{m}_{-1}^l + \mathbf{W}_u \mathbf{a}_{-1}^l \right) \right. \\ &\quad \left. + \mathbf{W}_u \mathbf{h}_{-1}^0 \right) \\ &= \operatorname{argmax} \left(\sum_{l=1}^L \left(\mathbf{W}_u \mathbf{W}_{\text{out}}^l \mathbf{O}_{-1}^l + \mathbf{W}_u \mathbf{a}_{-1}^l \right) \right. \\ &\quad \left. + \mathbf{W}_u \mathbf{h}_{-1}^0 \right), \end{aligned} \quad (6)$$

where $\mathbf{O}_{-1}^l = \sigma \left(\mathbf{W}_{\text{in}}^l \left(\mathbf{a}_{-1}^l + \mathbf{h}_{-1}^{l-1} \right) \right)$ is activation function output at the last token at layer l .

Following §2.2, we empirically focus on $\mathbf{W}_u \mathbf{W}_{\text{out}}^l \mathbf{O}_{-1}^l$ in Eq. 6 and omit the remaining parts. We regard o_i^l , the i -th element of \mathbf{O}_{-1}^l , as the activation of the i -th neuron at the last token at layer l , and $\mathbf{W}_u \mathbf{W}_{\text{out}}^l$ is considered as a new unembedding matrix at each layer. The function of $\mathbf{W}_u \mathbf{W}_{\text{out}}^l$ is to project the activation of the neurons onto a distribution of the token vocabulary, which is in accordance with the assumption in recent work (Geva et al., 2021; Ram et al., 2023; Schwettmann et al., 2023). The distributions at each layer then are summed up to obtain a final distribution, which contains the contributions of the all neurons across all layers within the model.

To evaluate the individual contribution of each neuron, we disassemble the multiplication of $\mathbf{W}_u \mathbf{W}_{\text{out}}^l$ and \mathbf{O}_{-1}^l as follows:

$$\mathbf{W}_u \mathbf{W}_{\text{out}}^l \mathbf{O}_{-1}^l = \sum \mathcal{T} \left(\mathbf{W}_u \mathbf{W}_{\text{out}}^l \cdot \mathcal{T} \left(\mathbf{O}_{-1}^l \right) \right), \quad (7)$$

where $\mathcal{T}(\cdot)$ is the transpose of the input matrix, and $\sum(\cdot)$ represents summing rows of the input.

Now we can see \mathbf{Q}^l in Eq. 7. We regard each element in \mathbf{Q}^l as a contribution score that each neuron contributes to each token, i.e., $\mathbf{Q}^l(i, j)$ indicates the score that the i -th neuron at layer l contributes to the j -th token. We can find that the score defined by Eq. 3 can commendably measure each neuron’s contribution to each token, which

proves our method is reasonable and theoretically supported.

It should be noted that while we can calculate scores for all tokens generated by the model, some tokens may not be readily discernible or describable from the image content alone. Therefore, for the purpose of clearer explanation, our analysis focuses only on tokens corresponding to nouns. If a noun consists of multiple tokens, we select the first token as being representative of that noun.

Based on Eq. 3, we compute the score of each neuron for every nominal token in the model output. Then we rank all the neurons across all layers within the model by the descending order and regard the top neurons as multi-modal neurons.

2.4 Tracing Focus of Neurons in Images

Previous works evaluate the correlation between the single neuron and semantics in the images (Bau et al., 2020; Hernandez et al., 2021) and analyse selectivity of neurons for specific visual concepts (Bau et al., 2017; Schwettmann et al., 2023) to characterize feature representations. Following their methods, we aim to evaluate whether our multi-modal neurons can identify particular feature regions in images. Accordingly, we are curious about where neurons focus their attention. To trace focus of neurons in images, we employ a visualization approach described below.

We denote the size of input images as $d_i \times d_i$ and rewrite the number of image patch tokens k as $d_t \times d_t$. We first take the activations of multi-modal neurons at image patch tokens and reshape them to $d_t \times d_t$. And then we scale them to $d_i \times d_i$ by bilinear interpolation. Now the scaled activations and the input images have the same size. For each image, we first plot a heatmap by using a mean scaled activation across top- k neurons and put it over the image. We then threshold the activations above the 95% percentile to produce a binary mask and also combine it with the original image.

2.5 Targeted Editing

Following previous works (Mitchell et al., 2022; Meng et al., 2022, 2023) on knowledge editing, we try to achieve a targeted editing from a source token t_0 to a target token t_1 when captioning. We propose an efficient algorithm to modify some of the model parameters (shown in Algorithm 1).

We denote top multi-modal neurons of source token t_0 as \mathcal{S} . For each multi-modal neuron $s_j \in \mathcal{S}$, we first get its location (l, i) , which means the i -th

Algorithm 1: Targeted Editing

Data: Source token t_0 , target token t_1 , neurons set \mathcal{S} , model \mathcal{M} , unembedding matrix \mathbf{W}_u , penalty weight β , learning rate α , epochs ϵ

Result: Edited model $\tilde{\mathcal{M}}$

```

1 for  $s_j \in \mathcal{S}$  do
2    $l, i \leftarrow$  location of  $s_j$ ;
3    $o_i^l \leftarrow$  activation function output of  $s_j$ ;
4    $\mathbf{w} \leftarrow$   $i$ -th row of  $\mathbf{W}_{\text{out}}^l$ ;
5    $\mathbf{v}_0 \leftarrow$   $t_0$ -th column of  $\mathbf{W}_u$ ;
6    $\mathbf{v}_1 \leftarrow$   $t_1$ -th column of  $\mathbf{W}_u$ ;
7   initialize  $\Delta\mathbf{w}$ ;
8    $\mathbf{w}' \leftarrow \mathbf{w} + \Delta\mathbf{w}$ ;
9   loss  $\leftarrow o_i^l(\mathbf{w}'\mathbf{v}_0 - \mathbf{w}'\mathbf{v}_1) + \beta \cdot \|\Delta\mathbf{w}\|_2$ ;
10   $\Delta\mathbf{w}^* \leftarrow$  gradient descent( $\Delta\mathbf{w}$ , loss,  $\alpha$ ,  $\epsilon$ );
11   $\tilde{\mathbf{W}}_{\text{out}}^l \leftarrow$  add  $\Delta\mathbf{w}^*$  to the  $i$ -th row of  $\mathbf{W}_{\text{out}}^l$ ;
12   $\tilde{\mathcal{M}} \leftarrow$  replace  $\mathbf{W}_{\text{out}}^l$  with  $\tilde{\mathbf{W}}_{\text{out}}^l$  in  $\mathcal{M}$ ;
end
13 return  $\tilde{\mathcal{M}}$ ;

```

neuron at layer l , and we pick out its activation function output o_i^l . Let \mathbf{w} be the i -th row of $\mathbf{W}_{\text{out}}^l$, \mathbf{v}_0 be the t_0 -th column of \mathbf{W}_u and \mathbf{v}_1 be the t_1 -th column of \mathbf{W}_u , respectively. We will modify \mathbf{w} by adding a $\Delta\mathbf{w}$ to get \mathbf{w}' .

Our goal is to make the probability of generating token t_1 higher than token t_0 , which is equivalent to make $o_i^l\mathbf{w}'\mathbf{v}_1$ larger than $o_i^l\mathbf{w}'\mathbf{v}_0$, so we define a loss function:

$$\text{loss} = o_i^l(\mathbf{w}'\mathbf{v}_0 - \mathbf{w}'\mathbf{v}_1) + \beta \cdot \|\Delta\mathbf{w}\|_2, \quad (8)$$

where β is penalty weight and $\|\Delta\mathbf{w}\|_2$ is a L_2 -norm constraint as a penalty to avoid the editing is too drastic and affects the generation of other tokens.

By applying Gradient Descent (Robbins and Monro, 1951), we acquire an optimal $\Delta\mathbf{w}$, denoted as $\Delta\mathbf{w}^*$. We then add $\Delta\mathbf{w}^*$ to the i -th row of $\mathbf{W}_{\text{out}}^l$ and replace the original $\mathbf{W}_{\text{out}}^l$ with the new $\tilde{\mathbf{W}}_{\text{out}}^l$ in model \mathcal{M} .

Notice that our algorithm is independent from the model, in other words, the solution procedure does not need to additionally train or infer the original model (the activation function output can be obtained when identifying neurons). Accordingly, this allows for efficient, timely and resource-efficient editing of the model parameters without retraining the entire network.

2.6 Evaluation Metrics

To comprehensively evaluate multi-modal neurons with quantitative indicators, we measure several evaluation metrics from multiple perspectives.

Semantic Sensitivity We hypothesize that multi-modal neurons exhibit sensitivity to certain concepts. Specifically, from a semantic perspective, they may be capable of representing the underlying meaning conveyed by text. To quantitatively evaluate the quality of their representations, we measure BERTScore (Zhang et al., 2020), BLEURT (Sellam et al., 2020) and MoverScore (Zhao et al., 2019). They can indicate the similarity between a noun and the top-10 tokens that corresponding neurons represent. We regard higher BERTScore, BLEURT and MoverScore as better semantic sensitivity.

Position Invariance When focusing on feature regions in images, multi-modal neurons ought to exhibit invariance irrespective of the input ordering. As such, we empirically evaluate their position invariance by shuffling the image patches. Specifically, for each noun in each image, we denote the original top- k multi-modal neurons as \mathcal{S}_k . We randomly shuffle the input sequence of image patches before sending to the LLM, and equally identify top- k multi-modal neurons, denoted as \mathcal{S}'_k . A high degree of similarity between \mathcal{S}_k and \mathcal{S}'_k indicates stronger position invariance. We calculate the ratio of invariant neurons before and after shuffling as below:

$$r_k = \frac{|\mathcal{S}_k \cap \mathcal{S}'_k|}{|\mathcal{S}_k|}, \quad (9)$$

and record a mean score across all images.

Cross-Images Invariance Besides position invariance, we also consider cross-images invariance. We randomly select N different images from the dataset that all contain a given noun c . Then, we separately identify the top- k neurons of these images and pick out neurons in common. We calculate the ratio of common neurons by:

$$s_{\text{CII}} = \frac{|\mathcal{S}_k^1 \cap \mathcal{S}_k^2 \cap \dots \cap \mathcal{S}_k^N|}{k}, \quad (10)$$

where \mathcal{S}_k^j is top- k multi-modal neurons of image j . The ratio of common neurons can indicate the cross-images invariance of the selected neurons.

Specificity We then evaluate the specificity of multi-modal neurons. We propose a metric $S@m$, which indicates the average score of top-1 multi-modal neuron to different concepts. Specifically, we pick out n images in the dataset, and separately identify their top-1 multi-modal neuron, denoted as \mathcal{S} , where $|\mathcal{S}| = n$. Each neuron can be represented as (l, i) , which means the i -th neuron at layer l . For

each neuron in \mathcal{S} , we provide a set of concepts T , where $|T| = m$, and calculate scores to each of them. Then we record a mean score across neurons in \mathcal{S} and concepts in T , denoted as $S@m$:

$$S@m = \frac{1}{n \cdot m} \sum_{(l,i) \in \mathcal{S}} \sum_{t \in T} s_{i,t}^l, \quad (11)$$

where $s_{i,t}^l$ is the contribution score calculated by Eq. 3, $n = |\mathcal{S}|$ and $m = |T|$.

To verify specificity, we choose two sets of concepts as T : related concepts and random concepts. The related concepts are with top probability to each neuron in \mathcal{S} , while random concepts are randomly selected from the vocabulary. If multi-modal neurons possess specificity, the metrics with related concepts will significantly outperform those with random concepts.

3 Experiments

3.1 Investigation Setup

We use LLaVA (Liu et al., 2023) and InstructBLIP (Dai et al., 2023) as our research models, two widely-use models for visual semantic understanding task. And we conduct experiments on SBU Captions Dataset (Ordonez et al., 2011), a dataset consists of more than 1 million images from Flickr. We compare our method with Multimodal Neurons (abbreviated as mmns) (Schwettmann et al., 2023), a technique for detecting *multimodal neurons* that map visual features to corresponding text, and uncovering the notions they introduce to the model’s residual stream. Furthermore, we establish a baseline (abbreviated as Base) that simply selects neurons with higher activations at the last token for basic comparison. Details about the implementations can be found in appendix A.1.

3.2 Identifying Multi-Modal Neurons

We employ methodology described in §2.3 to identify multi-modal neurons. Figure 2 shows the distribution of unique multi-modal neurons for 1000 images sampled from SBU. We can see that our neurons widely occur in higher layers, which is consistent with previous work (Liu et al., 2019; Wang et al., 2022). To further explore characteristics of the multi-modal neurons, we conduct a series of experiments based on them.

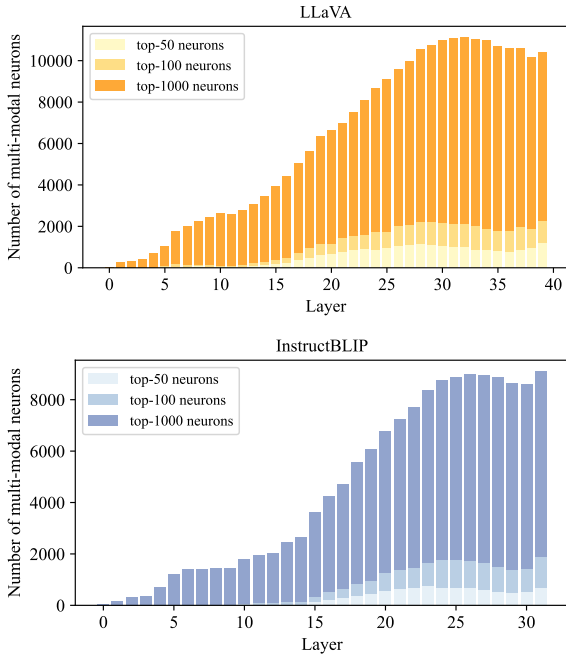


Figure 2: Distribution of unique multi-modal neurons per layer in LLaVA and InstructBLIP, chosen by different number of neurons with top contribution scores for each image.

3.3 Are Multi-Modal Neurons Sensitive to Certain Concepts?

We now discuss whether multi-modal neurons are sensitive to certain concepts in following parts: tracing focus of neurons in images (§3.3.1), determining textual meanings of neurons (§3.3.2), verifying position invariance (§3.3.3) and cross-images invariance (§3.3.4) of neurons.

3.3.1 Tracing Focus of Neurons in Images

Following previous works (Bau et al., 2017, 2020; Hernandez et al., 2021; Schwettmann et al., 2023), we trace the focus of our multi-modal neurons in images and evaluate whether they can identify particular feature regions in images.

We take the activations of multi-modal neurons at image patch tokens, and plot the heatmap and binary mask for each image. As InstructBLIP only have 32 image patch tokens, which prevents employing the aforementioned method, we only conduct experiments on LLaVA. Table 1 shows an example image. We can see that multi-modal neurons mainly focus on image regions that containing corresponding nouns, and pay less attention to other unrelated area. When increasing the value of k , the resultant heatmaps and binary masks exhibit only minor variations. They reliably highlight the

Image & Original output				
		LLaVA: a man wearing a yellow hat and smiling.		
Heatmap & Binary mask				
Noun	Heatmap & Binary mask			
	Top-1	Top-10	Top-100	Top-1000
man				
hat				

Table 1: Heatmap and binary mask results of an example image. We plot each heatmap by using scaled mean activations across top- k neurons, where $k = 1, 10, 100, 1000$, and plot binary mask by thresholding mean activations above the 95% percentile, respectively.

semantically pertinent areas throughout.

3.3.2 Determining Textual Meanings of Neurons

We then verify whether our multi-modal neurons can represent textual meanings. Considering the multiplication of the unembedding matrix and the second layer of FFN is regarded as a projection from the activation of the neurons to probability distributions of the token vocabulary, we empirically sort rows correspond to multi-modal neurons and pick out the top-10 tokens as each neuron represents. We report an example result compared with mmns and baseline in Table 2. We can find that the baseline and mmns choose the neurons that are hardly correlated with nouns, whereas our method can more precisely identify neurons representing semantic meanings in comparison to them. More examples are shown in appendix B.2.

To provide stronger evidence, we measure metrics of semantic sensitivity mentioned in §2.6, between the noun and each token that corresponding neurons represent. Table 3 shows the mean results

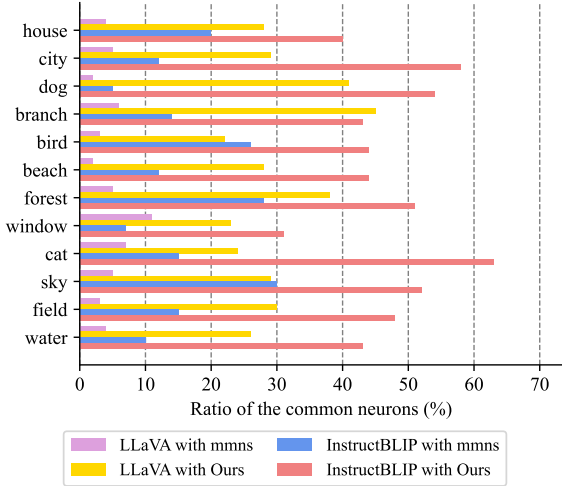
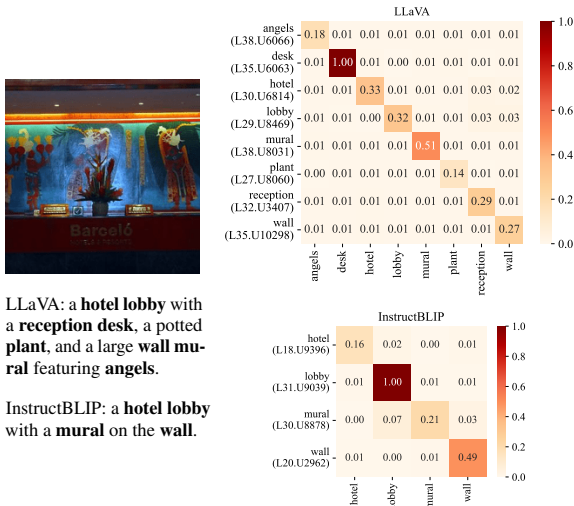


Figure 4: Ratios of the common neurons in top-100 neurons selected by mmns and our method. We set $N = 5$ and report results of some nouns that frequently appear in sampled images.



LLaVA: a hotel lobby with a reception desk, a potted plant, and a large wall mural featuring angels.

InstructBLIP: a hotel lobby with a mural on the wall.

Figure 5: Heatmap of the scores (after normalization) of multi-modal neurons corresponding to specific concepts when encoding different contents in an example image. The x-axis represents nouns in the given image, and y-axis represents the top-1 neuron corresponding to each noun, respectively. Darker blocks indicate higher scores, which means higher relevance.

icates our multi-modal neurons possess stronger position invariance.

3.3.4 Cross-Images Invariance of Neurons

In addition to position invariance, we also expect multi-modal neurons possess cross-images invariance, which means same neurons shall occur in different images carrying similar semantic information. To verify this, we employ the commonality score mentioned in §2.6. The re-

Model	Type	S@1	S@5	S@10	S@50
LLaVA	Related	3.549	2.920	2.333	0.467
	Random	0.018	0.012	0.014	0.003
InstructBLIP	Related	2.504	2.133	1.774	0.355
	Random	0.005	0.007	0.008	0.002

Table 4: Average scores that multi-modal neurons contribute to related concepts and random concepts. We report average scores with $m = 1, 5, 10, 50$, which are denoted as S@1, S@5, S@10 and S@50, respectively.

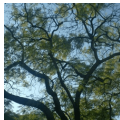
Image & Original output	
	LLaVA: a tree with many branches and leaves, set against a blue sky.
Noun	Model output
tree	a Hamon's Garden, featuring a Hamon' the S the Hamon's Garden, featuring a Hamon's the S the Hamon's ...
branches	ameshupelageaameshupelageaamesh...
leaves	a tree with branches spread out, surrounded by tree branches and Homosassa, Florida, and the things around it.
sky	a tree with leaves, possibly a palm tree, with a large and sturdy trunk, surrounded by a large, vibrant, and colorful body of leaves.
random	a tree with many branches and leaves, set against a blue sky.

Table 5: Perturbation results in LLaVA. For each noun in the image, we only perturb the top-5 multi-modal neurons. For comparison, we report a result of perturbing the same number of random chosen neurons.

sults of mmns and our method are shown in Figure 4. Our multi-modal neurons significantly outperform mmns both in LLaVA and InstructBLIP. Specifically, our method achieves common neuron ratios over 20% in LLaVA and mostly over 40% in InstructBLIP, which is substantially higher than mmns that attain ratios mainly under 10% in LLaVA and under 30% in InstructBLIP. We report more results with different N and k in appendix B.4.

3.4 Are Multi-Modal Neurons Specific?

For multi-modal neurons, merely exhibiting sensitivity is insufficient. If said neurons are sensitive to all concepts indiscriminately, this does not sufficiently demonstrate their functional role within the model. As such, we investigate whether these neurons exhibit specificity, such that they achieve significantly higher scores only when encoding visual features corresponding to a particular concept, with comparatively lower scores for unrelated image contents. We record the scores (see Eq. 3) of multi-modal neurons that correspond to their specific textual meanings when encoding other differ-


Image	Model	Target	Edited model output
 <p>LLaVA: a white cat sleeping in a tree. InstructBLIP: a white cat sleeping in a tree.</p>	LLaVA	monkey	a white monkey sleeping in a tree.
		clock	a clock clockwise, a clock on a tree, and a clock in a tree.
		iPhone	a white iPhone lying on a tree stump.
		food	a white food in a tree.
		computer	a white computer mouse resting on a tree branch.
	InstructBLIP	monkey	a white monkey sleeping in a tree.
		clock	a white clock sleeping in a tree.
		iPhone	a white iPhone 3Gs sitting on a tree stump.
		food	a white food sleeping in a tree.
		computer	a white computer sleeping in a tree.

Table 6: Targeted editing results of an example image. We choose noun *cat* from the original caption and transform it to 5 target nouns. Target nouns are in bold in the edited model output.




Source Noun: bird		
Image	Target	Edited LLaVA’s output
	None	a bird walking on the beach near the water.
	cat	a cat walking on the beach near the water.
	horse	a horse on the beach, walking through the water and enjoying the waves.
	None	a bird , possibly a pigeon, standing in a puddle of water on a city street.
	cat	a cat sitting in a puddle of water.
	horse	a horse in a pond, surrounded by leaves and water.
	None	a river flowing through a rocky area, with a waterfall and a rocky cliff.
	cat	a river flowing through a rocky area, with a waterfall and a rocky cliff.
	horse	a river flowing through a rocky area, with a waterfall and a rocky cliff.

Table 7: Edited LLaVA’s output of different images. We select *bird* as source noun, choose *cat* and *horse* as target noun (*None* means no editing), and modify model parameters based on image (a). We then test the edited model on another two images, where image (b) contains the source noun *bird* and image (c) doesn’t.

ent concepts in the same image. Figure 5 shows an example. Additional examples are provided in appendix B.5. We can see that when encoding a specific concept, the top-1 multi-modal neuron receives a higher score than irrelevant concepts. We also propose a metric to quantify the specificity of neurons (see §2.6). The results are shown in Table 4, from which we can find that neurons significantly get higher scores to those related concepts than to unrelated concepts. We conclude multi-modal neurons do not exhibit uniform activation, but rather demonstrate selectivity specifically corresponding to designated conceptual representations.

3.5 Do Multi-Modal Neurons Causally Affect Output?

We have demonstrated that multi-modal neurons display properties of sensitivity and specificity. We now seek to determine the extent to which they may affect the model’s predictions.

Perturbation Study Previous works (Mitchell et al., 2022; Meng et al., 2022, 2023) have shown that applying directional editing to transformer FFNs significantly change the model output. Inspired by these, we first try to perturb multi-modal neurons and compare with perturbing random neurons. Specifically, for each noun in each image, we add a Gaussian noise ($\mu = 0$ and $\sigma = 0.5$) to the i -th row of the second layer of FFN at layer l , where (l, i) is the position of each neurons in LLaVA. We can see that perturbing multi-modal neurons really makes a difference in model output, while simply perturb few random neurons has no impact on model. Furthermore, we notice that applying perturbation on neurons sometimes makes the corresponding token disappear in output and provides some new tokens, while sometimes results in meaningless output (e.g., in Table 5, when we perturb nouns ‘leaves’ and ‘sky’, the model can generate fluent output without containing ‘leaves’ and ‘sky’, but it is confused when we perturb nouns ‘tree’ and ‘branches’). The former phenomenon piques our curiosity regarding the potential possibility that a deliberate, nuanced alteration may substitute for Gaussian noise to enable targeted editing of model outputs. We aim to empirically validate this hypothesis in the subsequent experimental analysis.

Targeted Editing We hypothesize that replacing

the Gaussian noise with an elaborate alteration can achieve a targeted editing. Accordingly, we design an efficient algorithm (described in §2.5 and shown in Algorithm 1) that edits the weight of the second layer of FFN. The algorithm will instruct the model complete a transformation from generating a token to outputting another token. Table 6 shows an example of targeted editing, where we guide the model generate a different noun from the original noun. We find that the model drops the source noun and successfully generates the target noun, which did not appear in the original output. To prove effectiveness of our method, we test the edited LLaVA on other different images, as shown in Table 7. We can see that when we input another image that contains the same source noun, the edited LLaVA will identify it and generate the target noun, while an unrelated image will not be affected. We confirm that multi-modal neurons play an decisive role in the model when transforming image features into textual representations, and causally affect the model output.

4 Related Work

Finding Neurons in Deep Neural Networks

There has been growing interest in interpreting and analyzing the inner workings of deep neural networks. Prior works have sought to characterize what types of information are encoded in individual neurons. Koh et al. (2020) proposes a technique for identifying “concept neurons” that detect semantic concepts in vision models. Dai et al. (2022) discusses the discovery of “knowledge neurons” which encode specific commonsense knowledge automatically learned during pre-training, while Wang et al. (2022) proposes a method to identify “skill neurons” in pre-trained Transformer-based language models that are heavily involved in specific tasks. Recently, Schwettmann et al. (2023) introduces a procedure for identifying “multimodal neurons”, which explain how LLM convert visual representations into corresponding texts.

Analysing Transformer-based Models With the proposal of the Transformer (Vaswani et al., 2017) architecture, Transformer-based models have achieved state-of-the-art performance across many natural language processing tasks (Zhang et al., 2022; Chung et al., 2022; Li et al., 2022; Chowdhery et al., 2022) and attracted a large amount of studies. Prior works have focused on the function and mechanism of self-attention modules (Voita

et al., 2019; Clark et al., 2019; Hao et al., 2021), while some works emphasized the significance of feed-forward layers in Transformer (Press et al., 2020; Geva et al., 2021; Dai et al., 2022). Among these, some works have probed Transformer representations to quantify their encoding of linguistic information (Peters et al., 2018; Niven and Kao, 2019; Yun et al., 2019).

5 Conclusion

We propose a new method identify multi-modal neurons in transformer-based multi-modal LLMs. We highlight three critical properties of multi-modal neurons by four well-designed quantitative evaluation metrics through extensive experiments. We also introduce a knowledge editing approach based on the identified multi-modal neurons, achieves a targeted editing from a specific token to another designative token. It is our hope that this work furnishes illuminating perspectives on multi-modal LLMs and stimulates additional explanatory artificial intelligence studies emphasizing model interpretability. We also anticipate that our targeted editing method may inform future work in domains such as anonymization, compliance, and brand alignment.

Limitations

While this work provides new insights into interpreting multi-modal large language models, there are several limitations that should be acknowledged: (1) We only conduct experiments on LLaVA and InstructBLIP, while other Transformer-based model may also be possible to be explained by our multi-modal neurons. Besides the Transformer architecture, it is still unclear whether neurons exist in other multi-modal models based on different architectures and requires further explorations. (2) We only focus on neurons in feed-forward layers in Transformer and omit other parts like the neurons in self-attention heads, which may also contribute to identify image features and generate output. (3) When analysing multi-modal neurons, we only consider the role of a single neuron. We expect future works can explore how multiple neurons jointly influence the model. (4) Our targeted editing only achieve a transformation from a source token to another designative token, which is still insufficient, since there are a large amount of words consist of multiple tokens. Further addressing these limitations through broader and more methodologically

rigorous studies would help advance knowledge in interpretability of multi-modal large language models.

Acknowledgements

We acknowledge the support of GPU cluster built by MCC Lab of Information Science and Technology Institution, USTC.

References

- David Bau, Bolei Zhou, Aditya Khosla, Aude Oliva, and Antonio Torralba. 2017. [Network dissection: Quantifying interpretability of deep visual representations](#). In *Proceedings of the IEEE Conference on Computer Vision and Pattern Recognition (CVPR)*.
- David Bau, Jun-Yan Zhu, Hendrik Strobelt, Agata Lapedriza, Bolei Zhou, and Antonio Torralba. 2020. [Understanding the role of individual units in a deep neural network](#). *Proceedings of the National Academy of Sciences*, 117(48):30071–30078.
- Wei-Lin Chiang, Zhuohan Li, Zi Lin, Ying Sheng, Zhanghao Wu, Hao Zhang, Lianmin Zheng, Siyuan Zhuang, Yonghao Zhuang, Joseph E. Gonzalez, Ion Stoica, and Eric P. Xing. 2023. [Vicuna: An open-source chatbot impressing gpt-4 with 90%* chatgpt quality](#).
- Aakanksha Chowdhery, Sharan Narang, Jacob Devlin, Maarten Bosma, Gaurav Mishra, Adam Roberts, Paul Barham, Hyung Won Chung, Charles Sutton, Sebastian Gehrmann, et al. 2022. [Palm: Scaling language modeling with pathways](#). *arXiv preprint arXiv:2204.02311*.
- Hyung Won Chung, Le Hou, Shayne Longpre, Barret Zoph, Yi Tay, William Fedus, Eric Li, Xuezhi Wang, Mostafa Dehghani, Siddhartha Brahma, et al. 2022. [Scaling instruction-finetuned language models](#). *arXiv preprint arXiv:2210.11416*.
- Kevin Clark, Urvashi Khandelwal, Omer Levy, and Christopher D. Manning. 2019. [What does BERT look at? an analysis of BERT’s attention](#). In *Proceedings of the 2019 ACL Workshop BlackboxNLP: Analyzing and Interpreting Neural Networks for NLP*, pages 276–286, Florence, Italy. Association for Computational Linguistics.
- Damai Dai, Li Dong, Yaru Hao, Zhifang Sui, Baobao Chang, and Furu Wei. 2022. [Knowledge neurons in pretrained transformers](#). In *Proceedings of the 60th Annual Meeting of the Association for Computational Linguistics (Volume 1: Long Papers)*, pages 8493–8502, Dublin, Ireland. Association for Computational Linguistics.
- Wenliang Dai, Junnan Li, Dongxu Li, Anthony Meng Huat Tiong, Junqi Zhao, Weisheng Wang, Boyang Li, Pascale Fung, and Steven Hoi. 2023. [Instructblip: Towards general-purpose vision-language models with instruction tuning](#).
- Zhengxiao Du, Yujie Qian, Xiao Liu, Ming Ding, Jiezhong Qiu, Zhilin Yang, and Jie Tang. 2022. [GLM: General language model pretraining with autoregressive blank infilling](#). In *Proceedings of the 60th Annual Meeting of the Association for Computational Linguistics (Volume 1: Long Papers)*, pages 320–335, Dublin, Ireland. Association for Computational Linguistics.
- Jinhao Duan, Hao Cheng, Shiqi Wang, Chenan Wang, Alex Zavalny, Renjing Xu, Bhavya Kailkhura, and Kaidi Xu. 2023. [Shifting attention to relevance: Towards the uncertainty estimation of large language models](#). *arXiv preprint arXiv:2307.01379*.
- Yuxin Fang, Wen Wang, Binhui Xie, Quan Sun, Ledell Wu, Xinggang Wang, Tiejun Huang, Xinlong Wang, and Yue Cao. 2023. [Eva: Exploring the limits of masked visual representation learning at scale](#). In *Proceedings of the IEEE/CVF Conference on Computer Vision and Pattern Recognition (CVPR)*, pages 19358–19369.
- Xinyang Geng, Arnav Gudibande, Hao Liu, Eric Wallace, Pieter Abbeel, Sergey Levine, and Dawn Song. 2023. [Koala: A dialogue model for academic research](#). Blog post.
- Mor Geva, Roei Schuster, Jonathan Berant, and Omer Levy. 2021. [Transformer feed-forward layers are key-value memories](#). In *Proceedings of the 2021 Conference on Empirical Methods in Natural Language Processing*, pages 5484–5495, Online and Punta Cana, Dominican Republic. Association for Computational Linguistics.
- Yaru Hao, Li Dong, Furu Wei, and Ke Xu. 2021. [Self-attention attribution: Interpreting information interactions inside transformer](#). In *Proceedings of the AAAI Conference on Artificial Intelligence*, volume 35, pages 12963–12971.
- Evan Hernandez, Sarah Schwettmann, David Bau, Teona Bagashvili, Antonio Torralba, and Jacob Andreas. 2021. [Natural language descriptions of deep visual features](#). In *International Conference on Learning Representations*.
- Yuheng Huang, Jiayang Song, Zhijie Wang, Huaming Chen, and Lei Ma. 2023. [Look before you leap: An exploratory study of uncertainty measurement for large language models](#). *arXiv preprint arXiv:2307.10236*.
- Pang Wei Koh, Thao Nguyen, Yew Siang Tang, Stephen Mussmann, Emma Pierson, Been Kim, and Percy Liang. 2020. [Concept bottleneck models](#). In *Proceedings of the 37th International Conference on Machine Learning*, volume 119 of *Proceedings of Machine Learning Research*, pages 5338–5348. PMLR.

- Junnan Li, Dongxu Li, Silvio Savarese, and Steven Hoi. 2023. [BLIP-2: bootstrapping language-image pre-training with frozen image encoders and large language models](#). In *ICML*.
- Junnan Li, Dongxu Li, Caiming Xiong, and Steven Hoi. 2022. [BLIP: Bootstrapping language-image pre-training for unified vision-language understanding and generation](#). In *Proceedings of the 39th International Conference on Machine Learning*, volume 162 of *Proceedings of Machine Learning Research*, pages 12888–12900. PMLR.
- Haotian Liu, Chunyuan Li, Qingyang Wu, and Yong Jae Lee. 2023. [Visual instruction tuning](#). *arXiv preprint arXiv:2304.08485*.
- Nelson F. Liu, Matt Gardner, Yonatan Belinkov, Matthew E. Peters, and Noah A. Smith. 2019. [Linguistic knowledge and transferability of contextual representations](#). In *Proceedings of the 2019 Conference of the North American Chapter of the Association for Computational Linguistics: Human Language Technologies, Volume 1 (Long and Short Papers)*, pages 1073–1094, Minneapolis, Minnesota. Association for Computational Linguistics.
- Christopher Manning, Mihai Surdeanu, John Bauer, Jenny Finkel, Steven Bethard, and David McClosky. 2014. [The Stanford CoreNLP natural language processing toolkit](#). In *Proceedings of 52nd Annual Meeting of the Association for Computational Linguistics: System Demonstrations*, pages 55–60, Baltimore, Maryland. Association for Computational Linguistics.
- Kevin Meng, David Bau, Alex Andonian, and Yonatan Belinkov. 2022. [Locating and editing factual associations in gpt](#). *Advances in Neural Information Processing Systems*, 35:17359–17372.
- Kevin Meng, Arnab Sen Sharma, Alex J Andonian, Yonatan Belinkov, and David Bau. 2023. [Mass-editing memory in a transformer](#). In *The Eleventh International Conference on Learning Representations*.
- Jack Merullo, Carsten Eickhoff, and Ellie Pavlick. 2023. [Language models implement simple word2vec-style vector arithmetic](#).
- Eric Mitchell, Charles Lin, Antoine Bosselut, Chelsea Finn, and Christopher D Manning. 2022. [Fast model editing at scale](#). In *International Conference on Learning Representations*.
- Timothy Niven and Hung-Yu Kao. 2019. [Probing neural network comprehension of natural language arguments](#). In *Proceedings of the 57th Conference of the Association for Computational Linguistics*, pages 4658–4664, Florence, Italy. Association for Computational Linguistics.
- Catherine Olsson, Nelson Elhage, Neel Nanda, Nicholas Joseph, Nova DasSarma, Tom Henighan, Ben Mann, Amanda Askell, Yuntao Bai, Anna Chen, et al. 2022. [In-context learning and induction heads](#). *arXiv preprint arXiv:2209.11895*.
- Vicente Ordonez, Girish Kulkarni, and Tamara L. Berg. 2011. [Im2text: Describing images using 1 million captioned photographs](#). In *Neural Information Processing Systems (NIPS)*.
- Matthew E Peters, Mark Neumann, Luke Zettlemoyer, and Wen-tau Yih. 2018. [Dissecting contextual word embeddings: Architecture and representation](#). *arXiv preprint arXiv:1808.08949*.
- Ofir Press, Noah A. Smith, and Omer Levy. 2020. [Improving transformer models by reordering their sub-layers](#). In *Proceedings of the 58th Annual Meeting of the Association for Computational Linguistics*, pages 2996–3005, Online. Association for Computational Linguistics.
- Alec Radford, Jong Wook Kim, Chris Hallacy, Aditya Ramesh, Gabriel Goh, Sandhini Agarwal, Girish Sastry, Amanda Askell, Pamela Mishkin, Jack Clark, Gretchen Krueger, and Ilya Sutskever. 2021. [Learning transferable visual models from natural language supervision](#). In *Proceedings of the 38th International Conference on Machine Learning*, volume 139 of *Proceedings of Machine Learning Research*, pages 8748–8763. PMLR.
- Ori Ram, Liat Bezalel, Adi Zicher, Yonatan Belinkov, Jonathan Berant, and Amir Globerson. 2023. [What are you token about? dense retrieval as distributions over the vocabulary](#). In *Proceedings of the 61st Annual Meeting of the Association for Computational Linguistics (Volume 1: Long Papers)*, pages 2481–2498, Toronto, Canada. Association for Computational Linguistics.
- Herbert Robbins and Sutton Monro. 1951. A stochastic approximation method. *The annals of mathematical statistics*, pages 400–407.
- Sarah Schwettmann, Neil Chowdhury, Samuel Klein, David Bau, and Antonio Torralba. 2023. [Multimodal neurons in pretrained text-only transformers](#). In *Proceedings of the IEEE/CVF International Conference on Computer Vision*, pages 2862–2867.
- Thibault Sellam, Dipanjan Das, and Ankur Parikh. 2020. [BLEURT: Learning robust metrics for text generation](#). In *Proceedings of the 58th Annual Meeting of the Association for Computational Linguistics*, pages 7881–7892, Online. Association for Computational Linguistics.
- Hugo Touvron, Thibaut Lavril, Gautier Izacard, Xavier Martinet, Marie-Anne Lachaux, Timothée Lacroix, Baptiste Rozière, Naman Goyal, Eric Hambro, Faisal Azhar, et al. 2023a. [Llama: Open and efficient foundation language models](#). *arXiv preprint arXiv:2302.13971*.
- Hugo Touvron, Louis Martin, Kevin Stone, Peter Albert, Amjad Almahairi, Yasmine Babaei, Nikolay Bashlykov, Soumya Batra, Prajjwal Bhargava, Shruti

- Bhosale, et al. 2023b. [Llama 2: Open foundation and fine-tuned chat models](#). *arXiv preprint arXiv:2307.09288*.
- Ashish Vaswani, Noam Shazeer, Niki Parmar, Jakob Uszkoreit, Llion Jones, Aidan N Gomez, Łukasz Kaiser, and Illia Polosukhin. 2017. [Attention is all you need](#). *Advances in neural information processing systems*, 30.
- Elena Voita, David Talbot, Fedor Moiseev, Rico Senrich, and Ivan Titov. 2019. [Analyzing multi-head self-attention: Specialized heads do the heavy lifting, the rest can be pruned](#). In *Proceedings of the 57th Annual Meeting of the Association for Computational Linguistics*, pages 5797–5808, Florence, Italy. Association for Computational Linguistics.
- Xiaozhi Wang, Kaiyue Wen, Zhengyan Zhang, Lei Hou, Zhiyuan Liu, and Juanzi Li. 2022. [Finding skill neurons in pre-trained transformer-based language models](#). In *Proceedings of the 2022 Conference on Empirical Methods in Natural Language Processing*, pages 11132–11152, Abu Dhabi, United Arab Emirates. Association for Computational Linguistics.
- Qinghao Ye, Haiyang Xu, Guohai Xu, Jiabo Ye, Ming Yan, Yiyang Zhou, Junyang Wang, Anwen Hu, Pengcheng Shi, Yaya Shi, et al. 2023. [mplug-owl: Modularization empowers large language models with multimodality](#). *arXiv preprint arXiv:2304.14178*.
- Chulhee Yun, Srinadh Bhojanapalli, Ankit Singh Rawat, Sashank J Reddi, and Sanjiv Kumar. 2019. [Are transformers universal approximators of sequence-to-sequence functions?](#) *arXiv preprint arXiv:1912.10077*.
- Susan Zhang, Stephen Roller, Naman Goyal, Mikel Artetxe, Moya Chen, Shuohui Chen, Christopher Dewan, Mona Diab, Xian Li, Xi Victoria Lin, et al. 2022. [Opt: Open pre-trained transformer language models](#). *arXiv preprint arXiv:2205.01068*.
- Tianyi Zhang, Varsha Kishore, Felix Wu, Kilian Q Weinberger, and Yoav Artzi. 2020. [Bertscore: Evaluating text generation with bert](#). In *International Conference on Learning Representations*.
- Wei Zhao, Maxime Peyrard, Fei Liu, Yang Gao, Christian M. Meyer, and Steffen Eger. 2019. [MoverScore: Text generation evaluating with contextualized embeddings and earth mover distance](#). In *Proceedings of the 2019 Conference on Empirical Methods in Natural Language Processing and the 9th International Joint Conference on Natural Language Processing (EMNLP-IJCNLP)*, pages 563–578, Hong Kong, China. Association for Computational Linguistics.
- Deyao Zhu, Jun Chen, Xiaoqian Shen, Xiang Li, and Mohamed Elhoseiny. 2023. [Minigpt-4: Enhancing vision-language understanding with advanced large language models](#). *arXiv preprint arXiv:2304.10592*.

A Implementation Details

A.1 Identifying Multi-Modal Neurons

For model LLaVA (Liu et al., 2023), we choose the version whose base LLM is LLaMA-2-13B-Chat (Touvron et al., 2023b) and visual encoder is ViT-L/14 (Radford et al., 2021). Each input image is resized to (224, 224) and encoded into a sequence $[z_1, \dots, z_k]$ of dimensionality 1024, where $k = 256$. Then a projection layer transforms sequence $[z_1, \dots, z_k]$ into image prompts $[x_1, \dots, x_k]$ of dimensionality 5120. The image prompts will be concatenated into the textual prompts and received by LLaVA. In LLaVA’s textual prompts, we use “Describe the image in few words.” as query. Notice that for better captioning results, we add a text prefix “An image of” after the LLaVA’s prompts.

For model InstructBLIP (Dai et al., 2023), we choose the version that employs image encoder including ViT-g/14 (Fang et al., 2023) and a Q-former (Li et al., 2023), and adopt Vicuna-7B (Chiang et al., 2023) as the LLM. Similar to LLaVA, each image is encoded into a sequence $[z'_1, \dots, z'_q]$, where $q = 256$. And then the sequence is sent into the Q-former to get the extracted image features $[z_1, \dots, z_k]$ of dimensionality 768, where $k = 32$. Then a projection layer transforms sequence $[z_1, \dots, z_k]$ into image prompts $[x_1, \dots, x_k]$ of dimensionality 4096. The image prompts will be concatenated with the textual prompts “Describe the image in few words.” and also added by a text prefix “An image of”.

We use greedy search when generating captions for each image, which means the token with the highest probability will be selected at each step. We calculate the contribution score $s_{i,t}^l$ for each nominal token t in the generated caption, and rank all contribution scores across all layers within the model by the descending order to select top neurons as multi-modal neurons. To identify all nouns in the caption, we use Stanford CoreNLP (Manning et al., 2014), a tool for natural language processing in Java, by a python wrapper ¹.

We compare our method with Multimodal Neurons (Schwettmann et al., 2023), which calculates the attribution scores to select neurons. In their method, an attribution score is obtained for each image patch and neuron. For fair comparison in our experiments, we modify this by taking the maximum attribution score across patches for each neu-

¹https://github.com/Jason3900/corenlp_client

ron. This modification avoids unnecessary repetition while maintaining the interpretability of the neuron attributions.

Furthermore, we established a baseline approach that solely considers the activations of neurons at the final token as contribution scores, selecting those neurons exhibiting higher levels of activation as contributory neurons.

A.2 Targeted Editing

For most images, we empirically pick out the top-5 multi-modal neurons as \mathcal{S} , initialize $\Delta\mathbf{w}$ as $\mathbf{0}$, and set the learning rate α as 0.001, the iteration epochs ϵ as 1000 and the penalty weight β as 4, respectively.

B More Experiment Results

We report more experiment results and show more cases here to confirm our conclusion convincingly.

B.1 Tracing Focus of Multi-Modal Neurons

We report heatmap and binary mask results of examples in Table 8. Each heatmap is plotted by using scaled mean activations across top- k neurons, where $k = 1, 10, 50, 100, 500, 1000$, and each binary mask is plotted by thresholding mean activations above the 95% percentile, respectively.

B.2 Textual Representations of Multi-Modal Neurons

Table 9 shows examples randomly sampled from SBU. For each noun in the caption, we report its multi-modal neurons with their corresponding top-tokens and their contribution scores.

B.3 Position Invariance of Multi-Modal Neurons

In Table 10, we report some example results of captions and multi-modal neurons before and after shuffling the input sequence of image patches.

B.4 Cross-Image Invariance of Multi-Modal Neurons

To confirm the cross-image invariance of multi-modal neurons, in Figure 6, we report the ratio of the common neurons in top- k neurons across N images that contain the same nouns, where $N = 2, 3, 4, 5$ and $k = 10, 100, 1000$, respectively.

B.5 Specificity of Multi-Modal Neurons

To verify the specificity of multi-modal neurons, in Figure 7, we report some examples of the heatmap

of the scores of multi-modal neurons corresponding to specific semantics when encoding different semantics.

B.6 Perturbing Multi-Modal Neurons

We report results of perturbing top-5 multi-modal neurons and 5 randomly selected neurons in Table 11.

B.7 Targeted Editing

Table 12 shows additional examples of targeted editing results.

Image & Original output



LLaVA: a small **owl** perched on a **metal pole** in a grassy **field**.

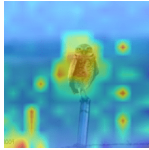
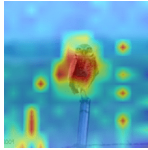
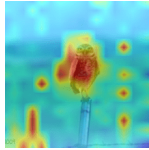
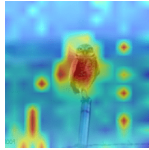
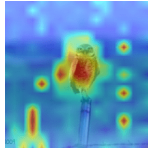
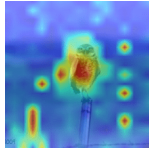






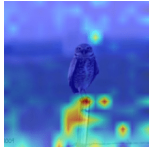
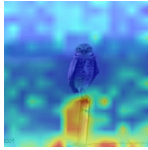
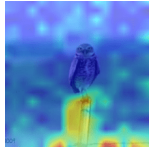
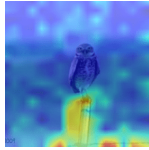
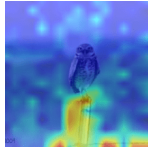
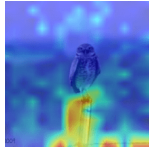






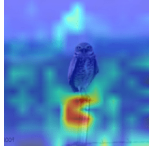
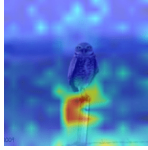
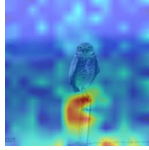
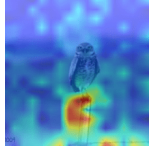
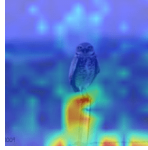
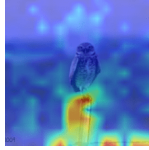

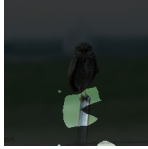
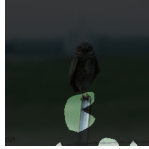
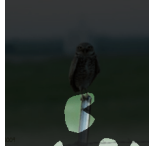


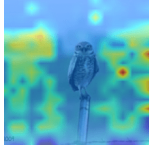
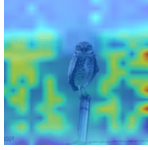
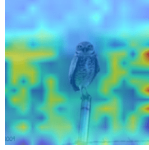
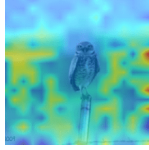
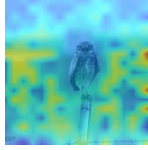
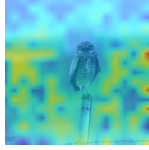
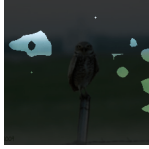
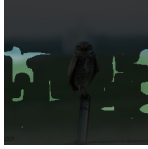
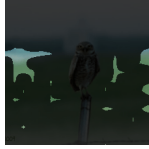



Noun	Heatmap & Binary mask					
	Top-1	Top-10	Top-50	Top-100	Top-500	Top-1000
owl						
						
metal						
						
pole						
						
field						
						

Image & Original output



LLaVA: a **box** filled with empty **beer bottles**, sitting on the **sidewalk**.



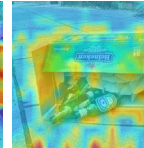
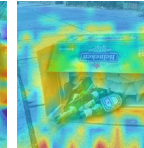
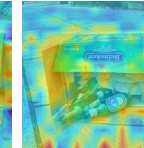
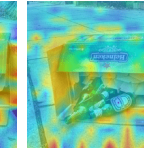








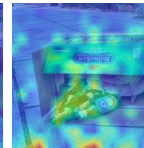
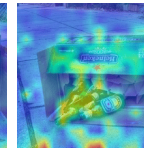
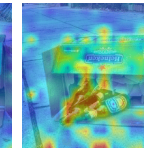
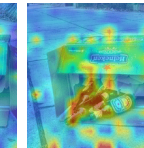






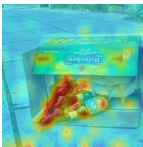
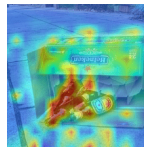
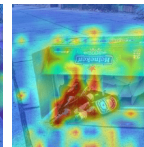
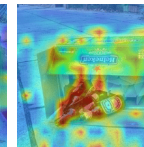
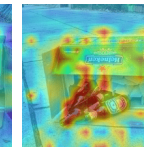
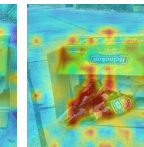








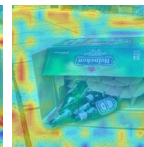
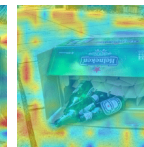
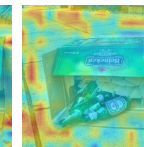
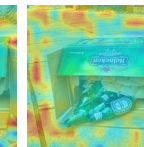






Noun	Heatmap & Binary mask					
	Top-1	Top-10	Top-50	Top-100	Top-500	Top-1000
box						
						
beer						
						
bottles						
						
sidewalk						
						

Image & Original output



LLaVA: a beautiful **lake** surrounded by **mountains**, with a **boat** floating on the **water**.

Noun	Heatmap & Binary mask					
	Top-1	Top-10	Top-50	Top-100	Top-500	Top-1000
lake						
mountains						
boat						
water						

Table 8: Heatmap and binary mask results of example images. We plot each heatmap by using scaled mean activations across top- k neurons, where $k = 1, 10, 50, 100, 500, 1000$, and plot binary mask by thresholding mean activations above the 95% percentile, respectively.

Image	Noun	Top neurons	Top tokens	Score
	man	L34.U3689	['man', 'man', 'Man', 'Man', 'MAN']	5.668
		L39.U12617	['man', 'manage', 'managed', 'managed', 'manager']	4.074
		L34.U6857	['man', 'man', 'Man', 'person', 'Mans']	1.932
		L28.U9293	['man', 'Man', 'Man', 'men', 'man']	1.869
		L22.U11069	['woman', 'lady', 'Woman', 'gentleman', 'girl']	0.743
	baby	L21.U9247	['baby', 'Baby', 'infant', 'dia', 'Bab']	2.908
		L22.U1178	['child', 'infant', 'ped', 'children', 'Children']	1.343
		L24.U2786	['child', 'elementary', 'Child', 'child', 'Child']	0.828
		L31.U2664	['children', 'kid', 'child', 'Children', 'Kid']	0.809
		L22.U10201	['born', 'baby', 'Baby', 'born', 'Born']	0.682
	arms	L24.U3244	['arms', 'bos', 'cust', 'lap', 'arm']	2.348
		L26.U2293	['hands', 'fingers', 'hand', '手', 'hand']	1.555
		L25.U824	['feet', 'arms', 'teeth', 'lap', 'mouth']	1.429
		L38.U10666	['arms', 'ar', 'arm', 'weapons', 'shoulders']	1.323
		L29.U9816	['arms', 'hands', 'lim', 'legs', 'eyes']	0.834
	boat	L28.U13532	['ship', 'ships', 'ship', 'vessel', 'ships']	3.387
		L24.U5729	['vehicle', 'vehicles', 'aircraft', 'boat', 'motor']	0.858
		L32.U1256	['fish', 'Fish', 'fish', 'marine', 'Marine']	0.762
		L18.U6783	['fish', 'marine', 'ocean', 'sea', 'aqu']	0.754
		L39.U5022	['ship', 'ship', 'ships', 'ships', 'кораб']	0.691
	bridge	L25.U6535	['bridge', 'brid', 'Bridge', 'bridge', 'crossing']	3.953
		L39.U7845	['bridge', 'Bridge', 'brid', 'bridge', 'Gate']	3.760
		L33.U10983	['Br', 'br', 'BR', 'BR', 'Br']	0.742
		L24.U11968	['bridge', 'covered', 'brid', 'shelter', 'Bridge']	0.789
		L39.U12961	['recon', 'brid', 'bridge', 'Bridge', 'bridge']	0.662
	day	L32.U13226	['Day', 'day', 'Day', 'day', 'DAY']	3.055
		L27.U13496	['day', 'Day', 'day', 'Day', 'days']	2.492
		L21.U8487	['day', 'days', 'day', 'today', 'dia']	1.642
		L34.U11066	['every', '日', 'day', 'afternoon', 'DAY']	1.599
		L23.U9634	['day', 'day', 'dia', 'Day', 'giorno']	1.534
	lake	L39.U1406	['water', 'water', 'Water', 'waters', '水']	1.017
		L19.U10352	['Lake', 'lake', 'ocean', 'river', 'waters']	0.963
		L27.U9679	['flo', 'Flo', 'rivers', 'river', 'River']	0.918
		L25.U6064	['Lake', 'Pool', 'pool', 'lake', 'pool']	0.764
		L24.U8137	['fresh', 'salt', 'Salt', 'aqu', 'lake']	0.675
	trees	L28.U9085	['branch', 'branches', 'Branch', 'branch', 'tree']	3.760
		L39.U4614	['Tre', 'tre', 'treat', 'tre', 'treated']	1.743
		L25.U5542	['grass', 'woods', 'leaf', 'forest', 'bush']	1.145
		L22.U171	['branches', 'branch', 'Branch', 'roots', 'root']	0.745
		L36.U1422	['tree', 'Tree', 'Tree', 'tree', 'trees']	0.637
	reflection	L39.U5565	['Ref', 'Ref', 'ref', 'ref', 'reflection']	2.908
		L31.U6067	['reflect', 'reflect', 'reflected', 'reflection', 'Mir']	2.736
		L26.U1358	['reflect', 'reflection', 'reflect', 'reflected', 'mirror']	1.856
		L30.U9652	['reflect', 'Mir', 'reflection', 'wing', 'reflect']	0.629
		L22.U5527	['reflect', 'reflection', 'reflect', 'reflected', 'catch']	0.488
water	L33.U3393	['water', 'water', 'Water', 'Wasser', '水']	4.148	
	L39.U1406	['water', 'water', 'Water', 'waters', '水']	4.008	
	L25.U4912	['water', 'water', 'sand', 'Water', 'snow']	1.511	
	L27.U11905	['tap', 'gall', 'water', 'running', 'filtered']	1.164	
	L18.U6783	['fish', 'marine', 'ocean', 'sea', 'aqu']	1.071	

LLaVA: a **man** holding a **baby** in his **arms**.

LLaVA: a **boat** sailing under a **bridge** on a cloudy **day**.

LLaVA: a calm **lake** with **trees** and a **reflection** of the trees on the **water**.





Image	Noun	Top neurons	Top tokens	Score
 <p>LLaVA: a star made out of paper or foil, hanging on a wall.</p>	star	L36.U12242	['star', 'Star', 'star', 'Star', 'stars']	4.605
		L23.U6095	['stars', 'star', 'Stars', 'star', '星']	1.155
		L35.U13549	['element', 'element', 'factor', 'step', 'component']	0.806
		L22.U13201	['Cross', 'cross', 'symbols', 'symbol', 'crossed']	0.610
	paper	L39.U7472	['ST', 'Stan', 'Stanley', 'Stuart', 'Sta']	0.497
		L29.U10814	['metal', 'concrete', 'steel', 'wood', 'iron']	1.168
		L25.U12448	['nap', 'Kle', 'matches', 'kle', 'match']	1.075
		L21.U4487	['paper', 'pap', 'paper', 'papers', 'pul']	0.915
		L34.U1584	['paper', 'paper', 'aper', 'papers', 'Pane']	0.775
	foil	L28.U271	['reads', 'reading', 'read', 'written', 'reader']	0.697
		L27.U2621	['wra', 'menu', 'boxes', 'pack', 'wrapping']	0.426
		L34.U11118	['leb', 'rolle', 'vere', 'Hoch', 'cco']	0.412
		L29.U10814	['metal', 'concrete', 'steel', 'wood', 'iron']	0.408
	wall	L34.U4464	['paint', 'Paint', 'aint', 'stuff', 'paste']	0.316
		L25.U5236	['Cook', 'cookies', 'cook', 'cot', 'pret']	0.305
		L35.U10298	['Wall', 'wall', 'wall', 'walls', 'alls']	3.846
L29.U9350		['Wall', 'wall', 'wall', 'walls', 'ana']	1.797	
L24.U11357		['wall', 'posted', 'walls', 'board', 'posting']	1.684	
 <p>LLaVA: a small red motorcycle parked on the grass near a beach.</p>	motorcycle	L24.U2145	['wall', 'wall', 'against', 'walls', 'Wall']	1.592
		L29.U2530	['steps', 'lad', 'steps', 'step', 'Lad']	1.114
		L34.U12567	['motor', 'Motor', 'mot', 'b', 'mot']	0.906
		L33.U6828	['mot', 'Mot', 'mot', 'motiv', 'Motor']	0.850
		L25.U11735	['motor', 'tennis', 'hockey', 'basketball', 'football']	0.641
	grass	L24.U5729	['vehicle', 'vehicles', 'aircraft', 'boat', 'motor']	0.591
		L27.U11389	['mot', 'motor', 'Mot', 'Motor', 'mot']	0.533
		L25.U5542	['grass', 'woods', 'leaf', 'forest', 'bush']	2.039
		L32.U12094	['grass', 'aupt', 'itza', 'ustration', 'inx']	1.873
		L30.U1365	['la', 'La', 'La', 'la', 'wn']	1.526
	beach	L20.U7408	['grass', 'garden', 'gard', '草', 'veget']	1.150
		L29.U7377	['gr', 'Gr', 'Grant', 'gr', 'grant']	1.145
		L36.U13537	['Coast', 'coast', 'beach', 'Beach', 'ocean']	2.984
		L30.U13327	['be', 'be', 'Be', 'BE', 'aches']	0.704
		L21.U13303	['beach', 'coast', 'Beach', 'Coast', 'shore']	0.607
 <p>LLaVA: a person walking through a snow-covered field or park.</p>	person	L21.U1114	['sw', 'Sw', 'sw', 'pool', 'Sw']	0.505
		L39.U11294	['flying', 'sea', 'aer', 'Sea', 'jet']	0.502
		L39.U12815	['person', '人', 'Person', 'person', 'persons']	2.531
		L31.U373	['person', 'Person', 'person', 'Person', 'personne']	2.254
		L31.U6487	['persons', 'personne', 'personas', 'Personen', 'Person']	2.004
	snow	L23.U7362	['human', 'bodies', 'body', 'humans', 'Body']	0.926
		L23.U5339	['member', 'worker', 'player', 'employee', 'politician']	0.880
		L39.U13129	['ski', 'Snow', 'snow', 'Ski', 'ski']	3.572
		L26.U13702	['fro', 'Fro', 'ice', 'free', 'Ice']	2.574
		L24.U10937	['rain', 'weather', 'Rain', 'snow', 'rain']	2.158
	field	L22.U395	['ski', 'snow', 'Ski', 'Snow', 'ski']	1.982
		L34.U11733	['winter', 'Winter', 'snow', 'January', 'February']	1.762
		L34.U12955	['fields', 'Field', 'field', 'fields', 'field']	3.416
		L25.U5542	['grass', 'woods', 'leaf', 'forest', 'bush']	0.714
L28.U1085		['garden', 'gard', 'Garden', 'Gard', 'grounds']	0.686	
park	L30.U1365	['la', 'La', 'La', 'la', 'wn']	0.609	
	L39.U7153	['materials', 'fields', 'fields', 'Fields', 'woods']	0.571	
	L39.U25	['park', 'par', 'par', 'park', 'club']	1.850	
	L31.U8282	['park', 'Park', 'park', 'bro', 'disp']	1.787	
	L28.U1085	['garden', 'gard', 'Garden', 'Gard', 'grounds']	1.785	
	L21.U3569	['square', 'Square', 'squares', 'cour', 'square']	0.584	
	L35.U12618	['university', 'inst', 'council', 'college', 'lake']	0.521	

Image	Noun	Top neurons	Top tokens	Score
	figurine	L36.U8273	['figure', 'Fig', 'Figure', 'figures', 'Fig']	2.572
		L24.U12276	['stat', 'statue', 'sculpt', 'Stat', 'stat']	1.161
		L18.U4770	['mini', 'figure', 'figures', 'figur', 'model']	1.014
		L38.U10971	['figure', 'figures', 'Figure', 'Fig', 'figured']	0.833
		L38.U2195	['Хронологија', 'Kontrola', 'konn', 'Audiod', 'techni']	0.627
	toy	L39.U98	['to', 'to', 'To', 'To', 'TO']	2.121
		L32.U6038	['Toy', 'To', 'Toast', 'TO', 'To']	1.298
		L39.U212	['', 'l', '-', '\n', '(']	1.101
		L38.U184	['to', 'to', 'To', '到', 'into']	0.890
		L39.U11820	['externas', '', 'a', '(', ',']	0.754
	model	L39.U3149	['models', 'model', 'models', 'model', 'Model']	2.893
		L23.U1705	['mini', 'model', 'models', 'model', 'Model']	1.705
		L24.U12276	['stat', 'statue', 'sculpt', 'Stat', 'stat']	0.914
		L18.U4770	['mini', 'figure', 'figures', 'figur', 'model']	0.710
		L39.U4397	['mode', 'Mode', 'Model', 'MODE', 'Mode']	0.639
surface	L37.U10337	['Sur', 'Sur', 'sur', 'surface', 'surfaces']	3.676	
	L30.U2704	['qu', 'sil', 'background', 'emb', 'Sil']	0.620	
	L36.U3279	['surface', 'face', '面', 'faces', 'fac']	0.492	
	L35.U8250	['surface', 'surfaces', 'superficie', 'superfic', 'повер']	0.439	
	L34.U6951	['soft', 'fi', 'bra', 'pla', 'soft']	0.438	
table	L23.U1705	['mini', 'model', 'models', 'model', 'Model']	0.458	
	L19.U13612	['tables', 'table', 'wall', 'sink', 'chair']	0.429	
	L26.U10793	['table', 'Table', 'tables', 'table', 'TABLE']	0.369	
	L32.U1205	['table', 'Table', 'Scanner', 'Table', 'table']	0.328	
	L18.U4770	['mini', 'figure', 'figures', 'figur', 'model']	0.321	
area	L35.U2653	['Area', 'area', 'area', 'Area', 'areas']	1.570	
	L31.U12802	['area', 'Area', 'zone', 'region', 'area']	0.630	
	L37.U2420	['region', 'region', 'regions', 'Region', 'Region']	0.494	
	L25.U12317	['places', 'cave', 'homes', 'environments', 'Places']	0.388	
	L31.U9217	['rug', 'car', 'blank', 'felt', 'fel']	0.332	
	plant	L27.U8060	['plant', 'Plant', 'plant', 'plants', 'planta']	1.087
		L29.U9056	['shr', 'bush', 'Bush', 'plant', 'plants']	0.962
		L28.U11440	['flow', 'blo', 'Flow', 'blo', 'Flow']	0.621
		L27.U498	['branch', 'Branch', 'branches', 'branch', 'bush']	0.600
		L25.U11504	['roots', 'root', 'Root', 'root', 'leaves']	0.502
	flowers	L28.U11440	['flow', 'blo', 'Flow', 'blo', 'Flow']	1.447
		L20.U11853	['flower', 'flowers', 'flor', 'Flor', '花']	1.277
		L27.U13027	['pet', 'pod', 'leaves', 'pet', 'bud']	0.990
		L27.U498	['branch', 'Branch', 'branches', 'branch', 'bush']	0.675
		L27.U3452	['fol', 'flowers', 'leaves', 'fol', 'leaf']	0.551
	flytrap	L39.U1989	['FI', 'fo', 'fig', 'fer', 'float']	0.913
		L36.U7481	['F', 'Ф', 'フ', 'Φ', 'Fest']	0.678
		L36.U6716	['file', 'フ', 'fake', 'flower', 'File']	0.625
		L28.U7379	['vol', 'flight', 'flow', 'fle', 'fl']	0.558
		L38.U998	['Fred', 'Frederick', 'Freder', 'Fon', 'Fen']	0.530
greenhouse	L30.U1994	['blo', 'green', 'Blo', 'blo', 'green']	2.258	
	L39.U3579	['red', 'green', 'red', 'yellow', 'blue']	1.122	
	L39.U9915	['white', 'silver', 'brown', 'blue', 'gold']	1.086	
	L28.U8699	['green', 'ho', 'Green', 'green', 'tunnel']	0.836	
	L29.U11697	['Green', 'Green', 'Blue', 'Brown', 'Black']	0.420	

LLaVA: a small **figurine**, possibly a **toy** or a **model**, is displayed on a green **surface**, possibly a **table** or a grassy **area**.

LLaVA: a **plant** with red **flowers** hanging from it, possibly a Venus **flytrap**, is displayed in a **greenhouse**.

Table 9: Multi-modal neurons with their corresponding top tokens and their contribution score. For each noun in the caption, we report top-5 neurons, each shown with the top-5 highest probability of tokens.

Image	Original	Shuffled
	<p>a tree with white flowers in a field, surrounded by a dirt road and a fence.</p> <p>tree: [L28.U9085, L36.U1422, L22.U171, L27.U8824]</p> <p>flowers: [L28.U11440, L20.U8129, L27.U13027, L27.U498]</p> <p>field: [L34.U12955, L28.U1085, L25.U5542, L39.U7153]</p> <p>dirt: [L39.U8730, L31.U526, L39.U212, L35.U1480]</p> <p>road: [L39.U8637, L26.U1456, L37.U12619, L29.U224]</p> <p>fence: [L27.U12313, L38.U5969, L37.U2453, L39.U212]</p>	<p>a tree with white flowers in a field, surrounded by a dirt road and a fence.</p> <p>tree: [L28.U9085, L36.U1422, L22.U171, L27.U8824]</p> <p>flowers: [L28.U11440, L20.U8129, L27.U13027, L27.U498]</p> <p>field: [L34.U12955, L28.U1085, L25.U5542, L39.U7153]</p> <p>dirt: [L31.U526, L39.U8730, L39.U212, L35.U1480]</p> <p>road: [L39.U8637, L26.U1456, L37.U12619, L29.U224]</p> <p>fence: [L27.U12313, L38.U5969, L37.U2453, L39.U212]</p>
	<p>a plate of meat, including steak and a side of vegetables, is presented.</p> <p>plate: [L33.U350, L23.U8551, L22.U9849, L19.U13764]</p> <p>meat: [L25.U9753, L29.U859, L23.U8551, L37.U11136]</p> <p>steak: [L37.U577, L25.U9753, L28.U10409, L22.U384]</p> <p>vegetables: [L37.U6234, L25.U3659, L38.U7433, L23.U8551]</p>	<p>a plate of meat, including steak and mashed potatoes, accompanied by a side of vegetables.</p> <p>plate: [L33.U350, L23.U8551, L22.U9849, L19.U13764]</p> <p>meat: [L25.U9753, L29.U859, L23.U8551, L22.U3753]</p> <p>steak: [L37.U577, L25.U9753, L28.U10409, L22.U384]</p> <p>vegetables: [L25.U3659, L37.U6234, L23.U8551, L25.U8838]</p>
	<p>a young girl standing in a doorway of a building, possibly a school, with a brick wall.</p> <p>girl: [L39.U5692, L28.U12204, L39.U364, L37.U9680]</p> <p>doorway: [L22.U9920, L27.U235, L21.U1052, L26.U10562]</p> <p>brick: [L29.U10814, L39.U8576, L25.U10651, L33.U10983]</p> <p>wall: [L35.U10298, L29.U9350, L29.U2530, L25.U10651]</p>	<p>a young girl standing in front of a stone wall, possibly a brick wall, with a doorway.</p> <p>girl: [L39.U5692, L28.U12204, L39.U364, L37.U9680]</p> <p>doorway: [L22.U9920, L29.U2530, L25.U5313, L25.U10438]</p> <p>brick: [L29.U10814, L24.U9050, L25.U10651, L33.U10983]</p> <p>wall: [L35.U10298, L29.U2530, L29.U9350, L19.U10353]</p>
	<p>a group of men in a room, celebrating and cheering while holding up their arms and fists.</p> <p>men: [L39.U5989, L29.U5763, L35.U8027, L29.U11953]</p> <p>room: [L38.U7800, L30.U6814, L29.U10611, L21.U8512]</p> <p>arms: [L23.U4494, L38.U10666, L24.U4501, L39.U5889]</p> <p>fists: [L38.U5969, L37.U2453, L39.U212, L36.U8631]</p>	<p>a group of men in a room, celebrating and cheering while holding up their arms and fists.</p> <p>men: [L39.U5989, L29.U5763, L35.U8027, L29.U11953]</p> <p>room: [L38.U7800, L30.U6814, L29.U10611, L21.U8512]</p> <p>arms: [L23.U4494, L38.U10666, L24.U4501, L26.U2293]</p> <p>fists: [L38.U5969, L37.U2453, L39.U212, L36.U8631]</p>
	<p>a man standing on a street corner, holding an Italian flag, and waving it while a police officer watches him.</p> <p>man: [L34.U3689, L39.U12617, L28.U9293, L34.U6857]</p> <p>street: [L39.U8140, L26.U1456, L26.U12900, L17.U5764]</p> <p>corner: [L38.U9436, L23.U12251, L28.U4161, L26.U8916]</p> <p>flag: [L25.U6794, L24.U6437, L23.U8268, L19.U12464]</p> <p>police: [L27.U7931, L31.U9142, L23.U2072, L35.U8410]</p> <p>officer: [L27.U7931, L23.U2072, L21.U3591, L39.U7884]</p>	<p>a man standing on a street corner, holding an Italian flag and waving it, while a police officer watches him from a car.</p> <p>man: [L34.U3689, L39.U12617, L28.U9293, L34.U6857]</p> <p>street: [L39.U8140, L26.U1456, L26.U12900, L17.U5764]</p> <p>corner: [L38.U9436, L23.U12251, L28.U4161, L26.U8916]</p> <p>flag: [L25.U6794, L19.U12464, L24.U6437, L23.U8268]</p> <p>police: [L27.U7931, L31.U9142, L23.U2072, L35.U8410]</p> <p>officer: [L27.U7931, L23.U2072, L21.U3591, L39.U7884]</p>

Table 10: Example results of captions and multi-modal neurons before and after shuffling the input sequence of image patches, respectively. We just record the nouns that appear both in original and shuffled captions from LLaVA, and for each noun, we report its top-4 multi-modal neurons.

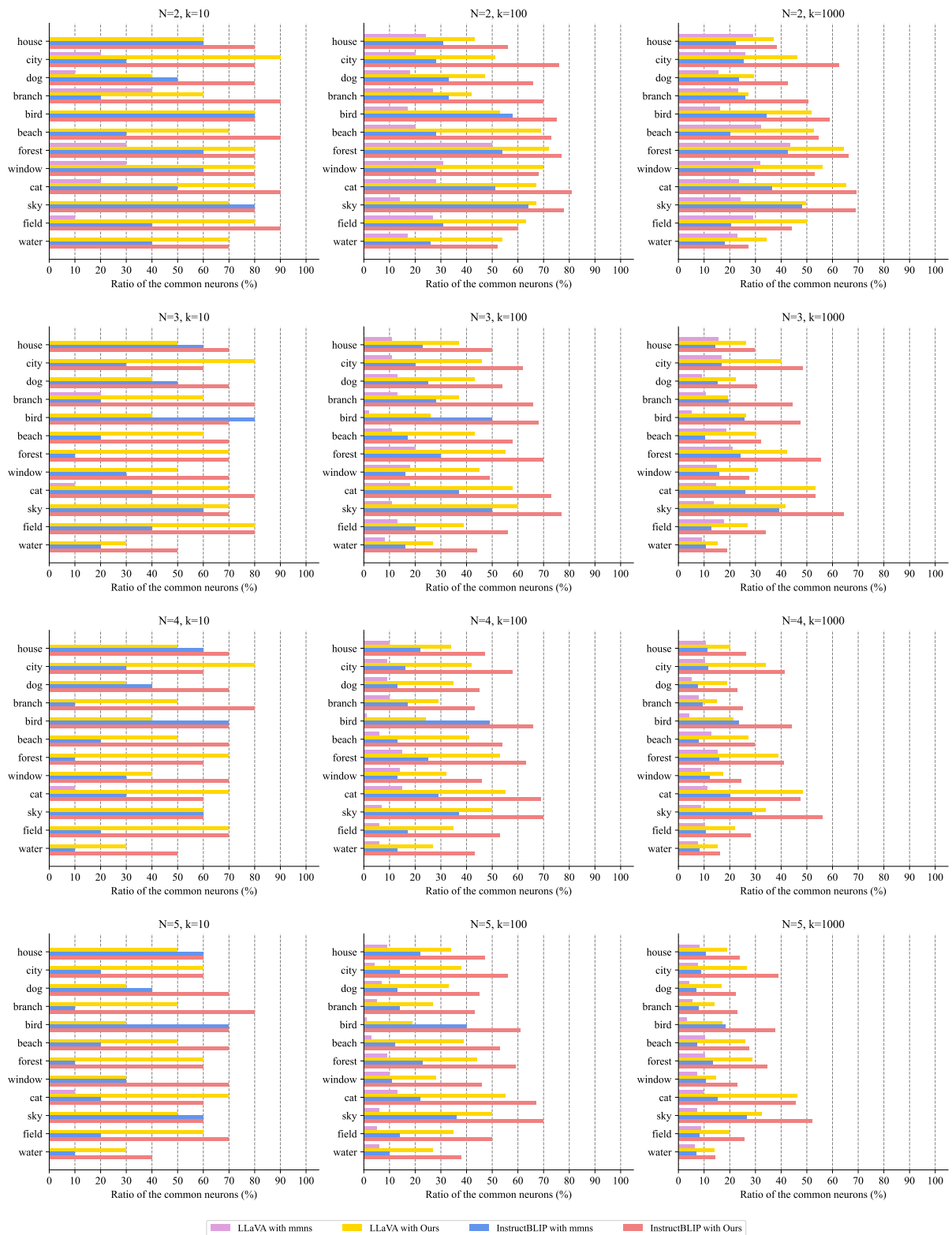
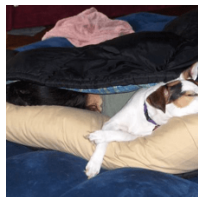
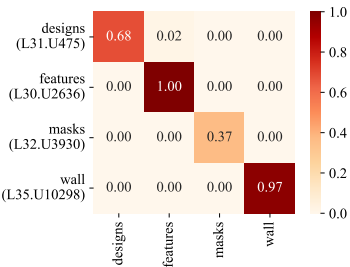


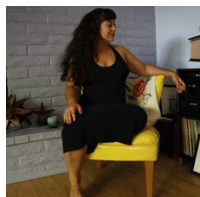
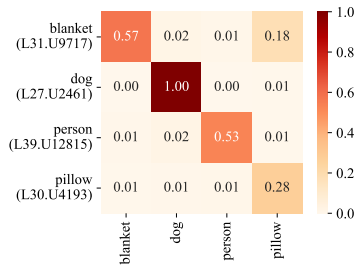
Figure 6: Ratio of the common neurons in top- k neurons selected by mmns and our method. We report $N = 2, 3, 4, 5$ and $k = 10, 100, 1000$ for model LLaVA and InstructBLIP.



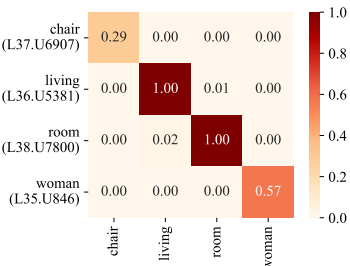
LLaVA: a wall covered with numerous masks, each with different facial features and designs.



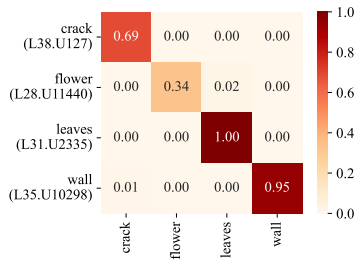
LLaVA: a dog sleeping on a pillow, with a person under a blanket nearby.



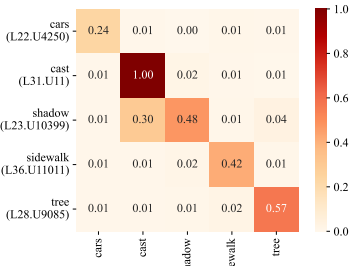
LLaVA: a woman sitting on a yellow chair in a living room.



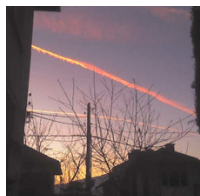
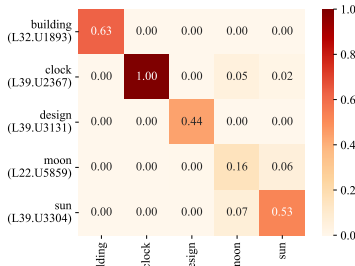
LLaVA: a pink flower with green leaves, growing out of a crack in a wall.



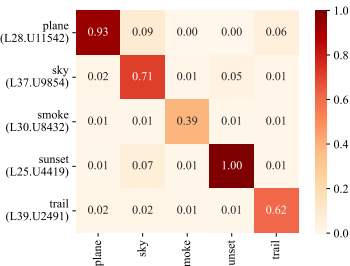
LLaVA: a tree with a shadow cast on the sidewalk, with cars parked nearby.



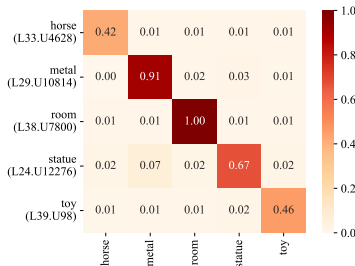
LLaVA: a large clock on a building, featuring a moon and sun design.



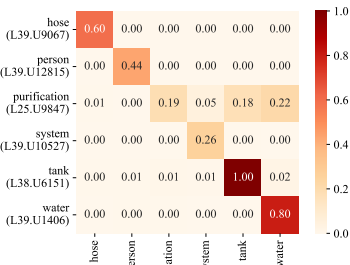
LLaVA: a sunset with a plane flying through the sky, leaving a trail of smoke behind it.



LLaVA: a horse statue or toy horse, possibly made of metal, is displayed in a room.



LLaVA: a person standing next to a large water tank, possibly a water purification system, with a hose attached to it.



LLaVA: a fish head with a large mouth and sharp teeth, possibly a pike, is displayed on a wooden table.

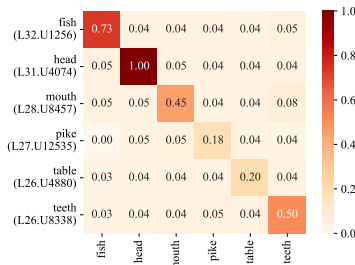


Figure 7: Heatmaps of the scores (after normalization) of multi-modal neurons corresponding to specific semantics when encoding different semantics. For each image, we report the result of the top-1 multi-modal neuron. In each heatmap, the x-axis represents nouns in the given image, and y-axis represents the top-1 neuron corresponding to each noun, respectively. Darker blocks indicate higher scores, which means higher relevance.

Image	Noun	Perturbed model output
 <p>LLaVA: a tall apartment building with balconies and a tree in the background.</p>	apartment	a multilevelishiigledishiigledishiigledishiigledishi...
	building	a white and blue building with a balcony and a tree in the background.
	balconies	a building with eradicated trees in the background, with eradicated trees on eradicated trees on 2200.
	tree	a white building with a balcony and a chair on it.
	background	a tall apartment building with balconies and a tree in front of it.
	random	a tall apartment building with balconies and a tree in the background.
 <p>LLaVA: a mountainous landscape with a village in the valley, featuring a grassy field and a road.</p>	landscape	a mountain range with a village in the valley, surrounded by a green field.
	village	a mountain with a small town or village located at its base, surrounded by a lush green field.
	valley	a mountain with a lush green field in the background, surrounded by a village.
	field	a mountain with a village in the valley below, surrounded by a lush green countryside.
	road	a mountainous landscape with a village in the valley, surrounded by a lush green field.
	random	a mountainous landscape with a village in the valley, featuring a grassy field and a road.
 <p>LLaVA: a large tower with a ball on top, standing next to a street light.</p>	tower	a large, white building with a light on a black background, with a lighted street lamp in the foreground.
	ball	a tall building with a light on top, possibly a light tower, and a street light nearby.
	street	a large white building with a clock tower, a street light, and a city skyline in the background.
	light	a tall tower with a large sphere on top, a building with a large sphere on top, and a building with a large sphere on top, all located in a city.
	random	a large tower with a ball on top, standing next to a street light.
 <p>LLaVA: a man hanging from a tree branch while wearing a hat.</p>	man	a person hanging from a tree branch, possibly participating in a tree-climbing activity or adventure.
	tree	a man hanging from a tree, possibly on a rope or a swing, with a sky background.
	branch	a man hanging from a suspended rope in a tree in the outdoors.
	hat	a person hanging from a tree branch, possibly participating in a ropes course or a similar activity.
	random	a man hanging from a tree branch while wearing a hat.

Table 11: Perturbation results of example images randomly sampled from SBU. For each noun in the image, we pick out top-5 multi-modal neurons and add a Gaussian noise to perturb them. We also report results of perturbing 5 randomly selected neurons for comparison.

Image	Source	Target	Edited model output
 <p>LLaVA: a small white dog standing on a tiled floor.</p>	dog	mouse	a mouse in a pink dress, standing on a tiled floor.
		bag	a white bag bag bag , or a white bag with a pink stripe, is standing on a tiled floor.
		dinosaur	a small white sauce dinosaur (dino) or a small white sauce-covered dinosaur toy is standing on a tiled floor.
	floor	baby	a baby white baby , wearing a pink dress, standing on a tiled floor.
		bed	a small white dog wearing a pink dress, standing on bed in a bedroom.
		chair	a small white dog wearing a pink dress, standing on chair in a chair , and looking at the camera.
		tree	a small white dog standing on a tree tree in a tree -lined area.
		beach	a small white dog, possibly a Maltese, wearing a pink dress and standing on the beach .
		table	a small white dog wearing a pink dress, standing on a table .
		ship	a small white dog standing on a ship shipment.
 <p>LLaVA: a man standing in a forest, surrounded by trees and a large rock.</p>	man	woman	a woman standing in a forest, surrounded by trees and rocks.
		baby	a baby in a forest, surrounded by trees and rocks.
		girl	a girl standing in a forest, surrounded by trees and rocks.
		stone	a stone wall or rock formation in a forest, with a stone cave or a rocky outcropping, and a stone wall with a stone door.
	forest	mountain	a man standing in a mountainous mountain area, surrounded by trees and rocks.
		garden	a man standing in a garden with a large rock and a tree.
		water	a man standing in a waterlogged area, surrounded by a waterfall and a rocky cliff.
		city	a man standing in a city park, surrounded by trees and a large rock formation.
		desert	a man standing in a deserted desert area, surrounded by trees and a large rock.
		hall	a man standing in a hallway of a cave, surrounded by rocks and trees.
	trees	wild	a man standing in front of a wild, wild rock formation, surrounded by wildlife and a forest trees.
		flowers	a man standing in a forest, surrounded by flowers and flowers in the background.
		cloud	a man standing in front of a cloudy sky, surrounded by a forest trees and cloudy sky.
		house	a man standing in a forest, surrounded by trees and a large house .
		tower	a man standing in a forest, surrounded by trees and a towering tower towering over him.
rock	building	a man standing in a forest, surrounded by trees and a large building .	
	ball	a man standing in a forest, surrounded by trees and a large ball of moss.	
	bear	a man standing in a forest, surrounded by trees and bushes, with a large bear bear nearby.	
	human	a man standing in a forest, surrounded by trees and a large human -like figure made of leaves.	



Image	Source	Target	Edited model output	
 <p>LLaVA: a red flower with a butterfly on it, sitting on a leafy plant.</p>	flower	head	a head of a red and white plant with a butterfly on it.	
		book	a red book with a white butterfly on it, placed on a bookshelf.	
		road	a red roadside plant with a white butterfly on it.	
		vehicle	a red vehicle with a white butterfly on top of it.	
		stream	a red and white flowering plant with a butterfly on stream .	
	butterfly	salt	a salt and pepper plant with a salt and pepper salt shaker on top of it.	
		insect	a flower with insect wings on it, sitting on a plant.	
		light	a light red flower with white petals, sitting on a leafy plant, and surrounded by light rain.	
	plant	rain	a red flower with rain drops on it, sitting on a leafy plant.	
		tree	a tree tree with a red flower and a butterfly on it.	
		wall	a red flower with a butterfly on it, sitting on a wall .	
		ground	a red flower with a butterfly on it, sitting on a ground with green leaves.	
		bowl	a red flower with a butterfly on it, sitting on a bowl bowl of water.	
		tower	a towering tower of red flowers planted in a towering tower of green towering tower .	
		park	a red flower with a butterfly on it, sitting on a park bench.	
		cup	a red flower with a butterfly on it, sitting on a cup .	
	 <p>LLaVA: a bridge over a body of water, with a boat passing underneath it.</p>	bridge	floor	a floor with a view of a floor , a car, and a floor with a view of a car.
			tree	a tree -lined road with a tree in the foreground, a tree in the middle, and a tree in the background.
			building	a building with a large building in the background, a boat on the water, and a building on the water.
			bed	a bed with a view of a bedroom and a bedroom window with a view of a bed .
water		hill	a hillside overlooking a hill with a hillside road and a hillside hill .	
		beach	a bridge over a beach , with a boat in the background and a car driving on the bridge.	
		heaven	a bridge over heavenly blue heaven , with a boat passing underneath it.	
		fire	a bridge over a large body of fire , with a boat in the background.	
		snow	a bridge over snowy mountains, with a boat traveling underneath it.	
		city	a bridge over a large body of city , with a boat visible in the distance.	
boat	plane	a bridge over a body of water, with a plane flying in the background.		
	vehicle	a bridge over a body of water, with a vehicle driving on it, and a vehicle on the other side of the bridge.		
	horse	a horse -drawn carriage traveling on a bridge over a body of water.		
	moon	a bridge over a body of water, with a moon in the background.		
	sun	a sunny day with a bridge over a body of water, with a sunny sky in the background.		

Table 12: Targeted editing results of example images sampled from SBU. For each source noun in the image, we artificially transform it to other target nouns. Target nouns are in bold in the edited model output.